RSC Advances




ROYAL SOCIETY OF CHEMISTRY

www.rsc.org/advances

RSC Advances

ARTICLE

# Pyridoxal-thiosemicarbazide: its anion sensing ability and application in living cells imaging

Received 00th January 20xx,
Accepted 00th January 20xx

DOI: 10.1039/x0xx00000x

www.rsc.org/

Darshna Sharma[a], Anuradha Moirangthem[b], Rajender Kumar[a], Ashok Kumar SK[c], Anil Kuwar[d], John F Callan[e], Anupam Basu[b,*], Suban K. Sahoo[a,f]*

A new anion selective chemosensor L was derived through a direct condensation reaction between pyridoxal and thiosemicarbazide. Sensor L showed selective recognition and sensing ability towards $F^-$ and $AcO^-$ anions through naked-eye detectable color change from colorless to light yellow, appearance of a new charge transfer absorption band at 404 nm and significant "turn-on" fluorescence at 506 nm. The detection limit of L as a fluorescent 'turn-on' sensor for the analysis of $F^-$ and $AcO^-$ was estimated to be 0.10 μM. The anion sensing mechanisms of L was supported with $^1$H NMR and DFT results. Finally, the cytoxicity effect of L and its ability to image intracellular $F^-$ ions in the living HeLa cells was investigated.

## Introduction

Substantial research has been focused on the development of colorimetric and fluorescent based chemosensors for the sensing of anionic species.[1-5] Owing to the high sensitivity, simplicity, real-time and on-line analysis of analytes, such chemosensors offer a great advantage over other conventional methods. Anions are widely distributed in the environment and biological systems, as exemplified by the acetate ion which has been found to be a possible tracer for malignancies and is extensively investigated in prostate cancer and its metastases.[6] Also, fluoride ion plays a significant role in the development of dental caries, clinical treatment for osteoporosis, toxicity resulting from its over accumulation in the bone and association with hydrolysis of the nerve gas sarin.[7] Therefore, the design and synthesis of fluorescence and colorimetric chemosensors for the selective detection of acetate and/or fluoride ions has attracted considerable attention in the field of supramolecular chemistry. In designing such chemosensors, the sensing of target anion is generally achieved by the coupling of two well-defined parts: one is the anion-binding part employing various H-donors functional groups such as pyrroles, urea/thiourea, guanidiniums, amides, phenol/catechol etc., and the second part is the signalling unit for the optical response.[8-11]

In this communication, we have developed a new Schiff base chemosensor (Z)-2-((3-hydroxy-5-(hydroxymethyl)-2-methylpyridin-4yl)methylene)hydrazinecarbothioamide (L) that comprises thiosemicarbazide as anion binding site coupled with a pyridoxal group acting as chromogenic/fluorescence unit for the selective sensing of bioactive anions (Scheme 1). The anion recognition ability of L towards $F^-$, $Cl^-$, $Br^-$, $I^-$, $HSO_4^-$, $H_2PO_4^-$ and $AcO^-$ was investigated by both spectroscopic (absorbance, fluorescence and $^1$H NMR) and density functional theory (DFT) methods. Finally, the sensor L was applied for the sensing of intracellular $F^-$ in live HeLa cells.

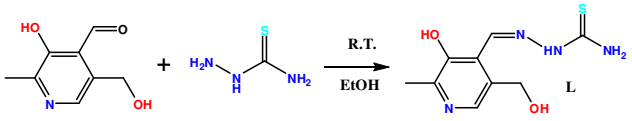


**Scheme 1.** Synthesis of the receptor L.

## Experimental

### Materials and methods

Unless otherwise specified, all reagents for synthesis were obtained commercially and used without further purification. In the titration experiments, all the anions were added in the form of tetra-n-butyl ammonium (TBA) salts, which were purchased from Spectrochem Pvt. Ltd., India or Acros Organic, and stored in a vacuum desiccator containing self-indicating silica and dried fully before using. Analytical grade DMSO and absolute ethanol were used. $^1$H NMR spectra were determined in DMSO-$d_6$ on a BRUKER AVANCE II 400 MHz NMR using TMS as an internal standard. Melting point was measured on digital melting point apparatus VMP-DS "VEEGO". UV-Vis spectra were recorded on a VARIAN CARY 50 spectrophotometer with a quartz cuvette (path length = 1 cm). The fluorescence spectra were recorded on the FluroMax-4 spectrometer.

A stock solution of the receptor L ($1.0 \times 10^{-4}$ M) and anions ($1.0 \times 10^{-3}$ M) were prepared in DMSO and $H_2O$. These solutions were

[a] Department of Applied Chemistry, S.V. National Institute of Technology (SVNIT), Surat, Gujarat, India. E-mail: suban_sahoo@rediffmail.com, Tel (Off.): +91-261-2201855.
[b] Molecular Biology and Human Genetics Laboratory, Department of Zoology, The University of Burdwan, Burdwan (WB), India. E-mail: abasu@zoo.buruniv.ac.in.
[c] School of Advanced Sciences, VIT University, Vellore (TN), India.
[d] School of Chemical Sciences, North Maharashtra University, Jalgaon, Maharashtra, India.
[e] School of Pharmacy and Pharmaceutical Sciences, The University of Ulster, Northern Ireland, BT52 1SA.
[f] Department of Applied Chemistry, Kyungpook National University, Daegu, 701-702, S. Korea.

†Electronic Supplementary Information (ESI) available: [details of any supplementary information available should be included here]. See DOI: 10.1039/x0xx00000x

used for different spectroscopic studies after appropriate dilution. For spectroscopic titrations, required amount of the receptor L (2 mL, $C_L$ = 5.0 ×$10^{-5}$ M) was taken directly into cuvette and spectra were recorded after successive addition of anion by using micropipette. The $^1$H NMR titration study was performed in DMSO-$d_6$ by adding different equivalents of TBAF into the solution receptor L (4 mM).

**Synthesis of receptor (L)**

Receptor L was synthesized according to Schiff base condensation.[12] First, the pyridoxal hydrochloride was desalted by adding KOH in methanolic medium. Then, the desalted pyridoxal (0.5 gm, 0.0024 mmol) was treated with thiosemicarbazide (0.21 gm, 0.0024 mmol) in methanol (25 ml). The yellow color precipitates were filtered and dried. $^1$H NMR (400 MHz, DMSO-$d_6$, $Me_4Si$, δ ppm): 11.55 (1H, s,-NH-), 9.57 (1H, br, Py-OH), 8.51 (1H, s, -CH=N), 8.28 and 8.05 (2H, s, -$NH_2$), 7.92 (1H, s, Py-H), 5.20 (1H, s, Py-$CH_2$-OH), 4.51 (2H, s, Py-$CH_2$-OH), 2.34 (3H, Py-$CH_3$).

**In vitro imaging**

HeLa cells procured from NCCS, Pune were grown in complete DMEM media supplemented with 10% FBS and 1% L-glutamine-penicillin-streptomycin. The cells were maintained at 37ºC in a humidified atmosphere with 5% $CO_2$. For the *in vitro* cellular imaging using the L.$F^-$ complex, the cells were seeded in 35mm cell culture dish with seeding density of 40X$10^4$ cells in 1ml complete DMEM media. Complete media was replaced with serum free media, after the cells have reached nearly 60% confluence. First, the cells were incubated with $F^-$ (8.73mM and 17.46mM) for approximately one hour so that the cells may take up the $F^-$ ions. The cells were then washed off properly to remove any unbound $F^-$ ions and incubated again with L (0.44mM) for nearly 16hrs. To remove any unbound L/$F^-$ complex formed, the cells were washed off with 1X PBS. Then the cells were observed under the fluorescence microscope using UV filter (340-380nm) (Leica DMI6000B). Through an attached CCD camera using image acquisition software (LAS V4.2) fluorescence images of the cells were captured. All the images were taken at 20X magnification.

**Cytotoxicity Assay**

To check any cytotoxic effect of the L/$F^-$ complex MTT assay was carried out. HeLa cells were seeded in 24 well culture plate with a seeding density of 10X$10^4$ cells per well in 500µL complete DMEM media. When the cells have reached nearly 60% confluence, complete media was replaced with serum free media and incubated the cells with NaF (8.73mM and 17.46mM) and L (0.44mM). The incubation time of the cytotoxicity assay was kept same as that of the cellular imaging. After incubating with both the L and NaF, the media was removed and added fresh serum free media. To all the wells 50µL of 3-(4,5-dimethylthiazol-2-yl)-2,5-diphenyltetrazolium bromide; thiazolyl blue [MTT, 5mg/mL PBS] was added and incubated for 3hrs. DMSO was added to dissolve the insoluble purple formazan product into a colored solution. The absorbance of the converted colored solution was measured spectrophotometrically at 590 nm.

## Results and discussion

The receptor (Z)-2-((3-hydroxy-5-(hydroxymethyl)-2-methylpyridin-4-yl)methylene)hydrazinecarbothioamide (L) was synthesized by a simple Schiff base condensation reaction of 3-Hydroxy-5-(hydroxymethyl)-2-methylpyridine-4-carbaldehyde with thiosemicarbazide (Scheme 1) and characterized by various spectroscopic techniques.[12] The anion recognition ability of L (1.0 × $10^{-5}$ M, in DMSO) was tested by naked-eye detection method and UV-Vis absorption spectroscopy in the presence of ten equivalents of different anions (TBA salts of $AcO^-$, $F^-$, $Cl^-$, $Br^-$, $I^-$, $HSO_4^-$ and $H_2PO_4^-$, in DMSO). The receptor L demonstrated a visually detectable color change from colorless to light yellow in the presence of $F^-$ and $AcO^-$ anions. No noticeable color change of L was observed upon addition of $Cl^-$, $Br^-$, $I^-$, $H_2PO_4^-$ and $HSO_4^-$ (Fig. 1 inset). The receptor L alone showed a strong absorption band centered at 332 nm due to π→π* transitions. Upon addition of $F^-$ and $AcO^-$, the receptor showed a new absorption band at 405 nm due to the formation of an anion-receptor complex through multiple intermolecular hydrogen bonds and/or the deprotonation of the polar–OH/NH groups of L (Fig. 1). The appearance of this new peak in the visible region may be assigned due to a possible internal charge transfer (ICT) process occurring between the receptor L and $F^-$/$AcO^-$ anions. Similar to $F^-$/$AcO^-$, the addition of $H_2PO_4^-$ also perturbed the absorption spectrum of L but the peak intensity at 405 was much lowered compared to $F^-$ and $AcO^-$. Other tested anions ($Cl^-$, $Br^-$, $I^-$, and $HSO_4^-$) showed no significant spectral changes of L.

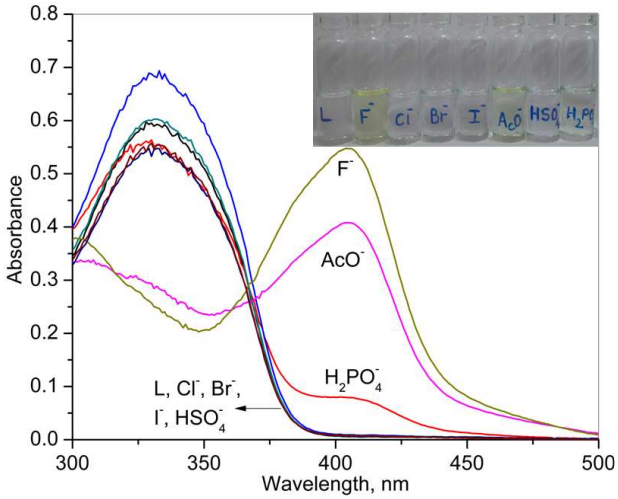


**Fig. 1.** UV-Vis absorption spectral changes of L (1.0 × $10^{-5}$ M) upon addition of ten equivalents of different anions in DMSO. Inset shows the color change of vials.

Given the selectivity of L for $F^-$ and $AcO^-$, the range over which it could detect these anions was then determined by performing the absorption titrations upon successive incremental addition of $F^-$ and $AcO^-$. As shown in Fig. 2 and Fig. S1, similar spectral changes of L was observed upon addition of both the anions indicating the similar recognition modes. Upon incremental addition of $F^-$/$AcO^-$ anions, the intensity of receptor band at 332 nm was decreased and concomitantly the charge transfer band at 405 nm was appeared with the formation of an isosbectic point at 369 nm. The isosbestic point indicates the equilibrium point between the receptor L and the new species (L.$F^-$/$AcO^-$) formed due to host-guest interaction with anions. The spectroscopic titrations data were examined by applying the Benesi-Hildebrand (B-H) equation to determine the binding constants (K) of the receptor-anion complexes.[13] From the B-H plots (inset Fig. 2 and Fig. S2), the binding constant of L for $F^-$ (2.27 × $10^4$ $M^{-1}$) was found to be similar to that of the $AcO^-$ (1.20 × $10^4$ $M^{-1}$). Also, the B-H plots along with the Job's plot (Fig. S3) clearly delineated the formation of 1:1 host-guest complex between receptor L and $F^-$/$AcO^-$.

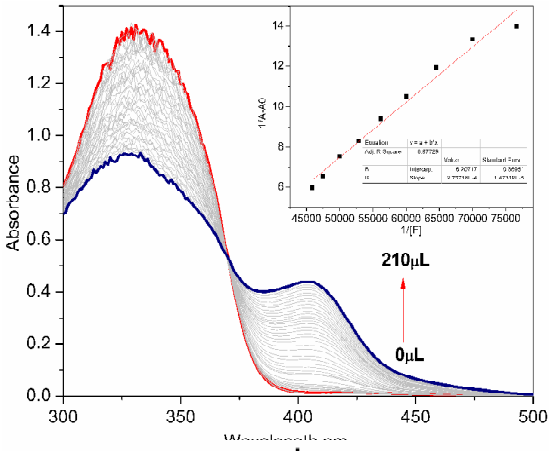


**Fig. 2.** Changes in the absorbance spectrum of L ($5.0 \times 10^{-5}$M) upon addition of incremental amounts of TBAF (0 μL to 210 μL, $1.0 \times 10^{-4}$ M) in DMSO. Inset showing the B-H plot.

The host-guest interaction between L and anions was further established by $^1$H NMR titration of L in the absence and presence of different equivalents TBAF in DMSO-$d_6$ (Fig. 3). The receptor peaks due to pyridoxal-OH (Py-OH) at 9.57 ppm and –NH- at 11.55 ppm were respectively disappeared and shifted downfield upon addition of 1 equivalent of TBAF with the appearance of a new peak at 14.44 ppm, which supported the deprotonation of L and formation of bifluoride ($HFH^-$). The interaction of amine-$NH_2$ with $F^-$ was also evidenced from the shifting of peaks from 8.28 and 8.05 ppm to 6.11 m and 8.61 ppm, respectively. Apparent structural changes in L upon interaction with $F^-$ can also be deduced from the shifting of the peaks due to imine-H, Py-H, Alc-OH and $–CH_2$- protons. In addition, due to the presence of multiple polar-NH/OH groups, the hydrogen bonded host-guest interaction between L and $F^-$ appeared to be continued even after the deprotonation of the Py-OH and –NH- protons. To confirm the partial deprotonation of L, the absorption spectrum of L was recorded by adding ten equivalents of TBAOH in DMSO (Fig. S4). Under similar condition, addition of TBAOH also generated an absorption band at 405 nm but the intensity was comparably lowered as observed with the fluoride anions. The above results clearly demonstrated that the sensing anions are functioning here as a base, giving rise to the partial deprotonation of the most acidic protons of L.

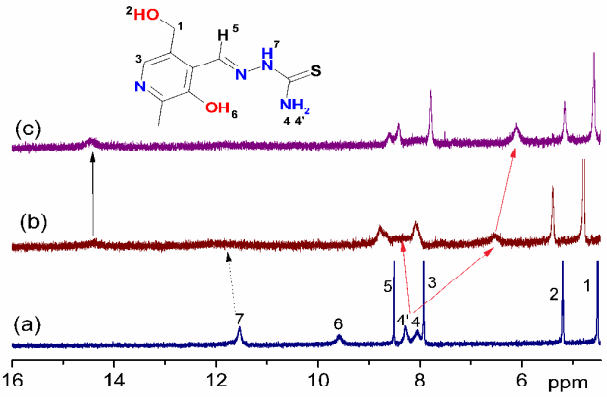


**Fig. 3.** $^1$H NMR spectra of L in absence (a) and presence of one (b) and three (c) equivalents of TBAF in DMSO-$d_6$.

The structural optimization of L and its deprotonated form were performed at B3LYP/6-31G(d,p) level by using the computational code Gaussian 09W[14] to complement the experimental evidences. Receptor L preferred an enolimine form with a strong intramolecular hydrogen bond of length 1.790 Å between the imine-N and Py-OH. The calculated Mulliken's atomic charges inferred that the protons of groups -$NH_2$, -NH-, Py-OH and alc-OH possessed the most positive charges of 0.264, 0.259, 0.378 and 0.311, respectively. Also, the analysis of molecular electrostatic potential (MEP) map of L (Fig. 4a) indicates that the most positive region shown in blue color are located on the polar-OH/–NH groups, which can interact with the anions as verified by $^1$H NMR titrations. Furthermore, the changes in the electronic properties of L and its deprotonated form were compared. Upon deprotonation of the Py-OH group of L, the band gaps ($\Delta E = E_{LUMO}$-$E_{HOMO}$) between the HOMO and LUMO of L was lowered from 0.146 eV to 0.118 eV. Also, the TDDFT results inferred that the receptor L gave maximum absorbance at 348 nm whereas the mono-deprotonated form of L had a maximum absorbance at 429 nm. The red-shifted absorbance of L upon deprotonation was analyzed from their HOMO and LUMO diagrams, which indicate the possible internal charge transfer process occurred due to the deprotonation of Py-OH group (Fig. 4b,c).

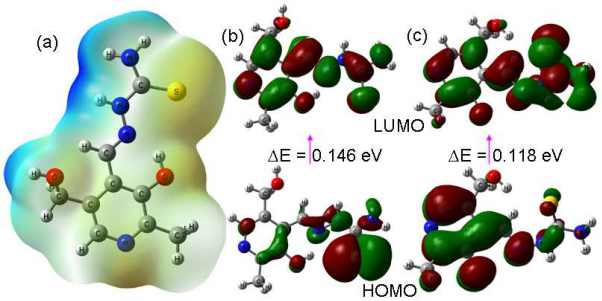


**Fig. 4.** DFT computed structure of the receptor L showing the (a) MEP and the frontier molecular orbitals (HOMO and LUMO) diagrams of (b) L and (c) its deprotonated form $L^{1-}$.

The anion sensing ability of the receptor L ($1.0 \times 10^{-5}$ M, DMSO) was also examined by fluorescence spectroscopy (Fig. 5). The free receptor L showed an emission band at 465 nm ($\lambda_{exc}$ = 335 nm). The fluorescence of L was selectively and distinguishably enhanced at 506 nm in the presence of $F^-$ and $AcO^-$. The fluorescence enhancement occurred due to the inhibition of the excited state intramolecular proton transfer (ESIPT) process due to the deprotonation of the py-OH group upon interaction with the most basic anions $F^-$/$AcO^-$. No noticeable changes in the fluorescence of L were observed with other examined anions such as $Cl^-$, $Br^-$, $I^-$, $HSO_4^-$ and $H_2PO_4^-$. The competitive experiments of L were conducted in the presence of 1 equiv. of $F^-$/$AcO^-$ mixed with 2 equiv. of other interfering anions. It was observed that the fluorescence profile of L was unaffected by other anions except $F^-$ and $AcO^-$ (Fig. S5 and S6). These results indicate that the receptor L has a good selectivity and specificity towards $F^-$ and $AcO^-$.

The limit of detection (LOD) was determined through fluorescence titrations of L with incremental addition of $F^-$ (Fig. 6) and $AcO^-$ (Fig. S7) in DMSO. Upon progressive addition of $F^-$ (0-9 equivalents), the fluorescence emission intensity at 506 nm was gradually enhanced. From fluorescence titration data (Fig. 6 inset and Fig. S8), the detection limit ($3\sigma/S$) of the receptor L as a

fluorescent 'turn-on' sensor for the analysis of $F^-$ and AcO- was estimated to be 0.10 μM. The obtained detection limit was far better than the permissible limit of $F^-$ in drinking water according world health organization (WHO).[15]

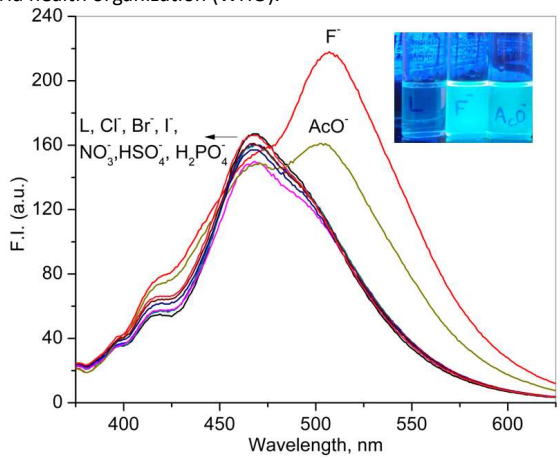


**Fig. 5.** Changes in the emission spectrum of L ($1.0 \times 10^{-5}$ M) on addition of equivalent amount of different anions in DMSO. Inset showing the color change under UV light, 365 nm.

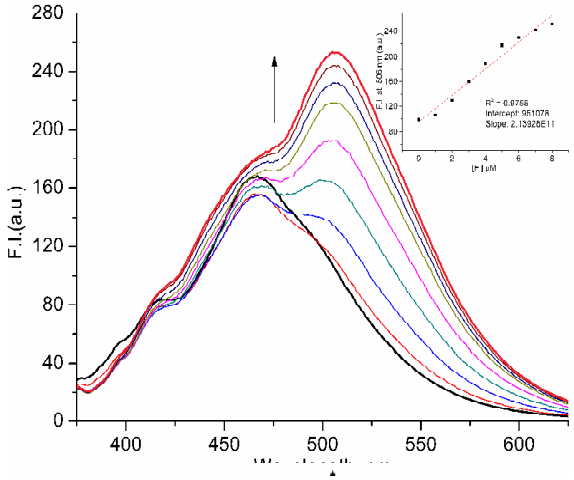


**Fig. 6.** The fluorescence titration of L ($1.0 \times 10^{-5}$ M) on incremental addition of $F^-$ (0-160 μL, $1.0 \times 10^{-4}$M) in DMSO. Inset showing the linear curve fitting of fluorescent intensity at 506 nm as a function of [$F^-$].

The detection of inorganic anions by L in aqueous medium was also investigated, as most practical applications would require this probe to operate in this medium. For this experiment, the receptor L was again dissolved in DMSO but the anions were added from their pure aqueous solution. This involved addition of 100 μL of different anions ($1.0 \times 10^{-4}$ M) into the receptor L (2 mL, $1.0 \times 10^{-5}$ M) solution which resulted in a naked-eye detectable color change under normal day light and UV irradiation (Fig. 7). The fluorescent 'turn-on' anions ($F^-$ and $AcO^-$) of L in aqueous medium encouraged us to study the imaging ability of intracellular fluoride in live cells. *In vitro* cellular imaging experiments were performed using the cervical HeLa cancer cell line to examine the ability of L to detect intracellular $F^-$ ions (Fig. 8). Cells were first treated with the required concentration of $F^-$ ions (8.73 mM and 17.46 mM) in PBS, cells washed with PBS and then treated with L (0.44 mM). Cells were again washed and then imaged using a fluorescence microscope. Control cells treated with L only or $F^-$ ions only were used as comparison. The resulting images, shown in Fig 8 reveal that cells treated with $F^-$ ions or L alone showed only background fluorescence while cells treated with both L and fluoride ions clearly showed cellular fluorescence, with the intensity greater for those treated with the higher concentration of $F^-$ ions. These results suggest that L showed potential to detect intracellular $F^-$ ions, however, the cellular fluorescence in imaging application of L in the presence of $F^-$ is influenced due to the competing nature of water.

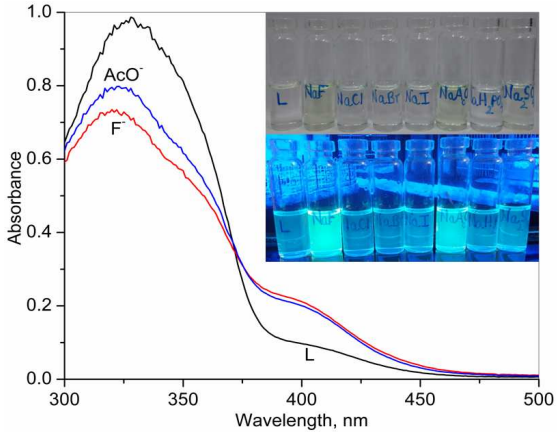


**Fig. 7.** UV-Vis absorption spectral changes of L ($1.0 \times 10^{-5}$ M) upon addition of anions. Inset shows the colour change upon addition of equivalent amount of different anions and under UV lamp.

From the MTT assay, it was revealed that the viability of the cells were unaffected by either L or L in the presence of $F^-$ ions. Even when viability was tested using twice the concentration of $F^-$ than that used in the imaging experiments only a minor reduction in viability was observed. Therefore, L demonstrates excellent biocompatibility in living cells and could potentially find use as an intracellular probe for $F^-$ ions (Fig. 9).

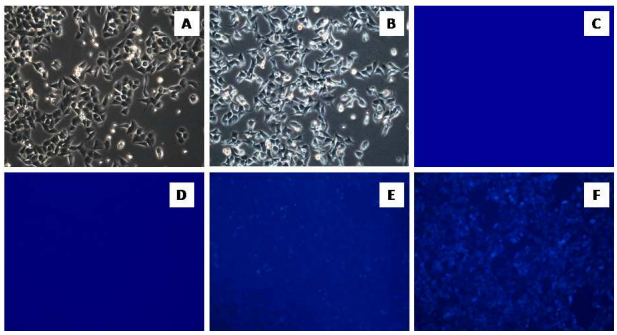


**Fig. 8.** Fig. A) Phase contrast image of the control cells; B) Phase contrast image of the cells incubated with $F^-$ (17.46 mM) and L (0.44 mM); C) Fluorescence image of the cells after incubating with $F^-$ (17.46 mM) only, as observed through UV filter; D) Fluorescence image of the cells after incubating with L (0.44 mM), as observed through UV filter; E) Fluorescence image of the cells after incubating with $F^-$ (8.73 mM) and L (0.44 mM), as observed through UV filter; F) Fluorescence image of the cells after incubating with $F^-$ (17.46 mM) and L (0.44mM), as observed through UV filter. (All the

images were taken at 20X magnification through an attached CCD camera using image acquisition software, LAS V4.2).

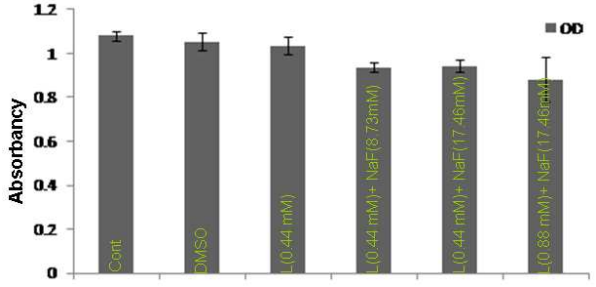


**Fig. 9.** The result of MTT assay after the cells were treated with L (0.44 mM and 0.88 mM) and $F^-$ (8.73 mM and 17.46 mM) for 16 hrs. The absorbance of the colored formazan product was measured spectrophotometrically at 590 nm. The decrease in the viability of the cells after the incubating the cells with the L/$F^-$ complex was not remarkable in comparison to the control cells.

## Conclusions

In conclusion, we have developed a new chemosensor containing vitamin $B_6$ cofactor pyridoxal as signaling unit for the selective detection of $F^-$ and $AcO^-$. Sensor L portrayed naked-eye detectable colorimetric changes under day and UV-light. It displayed a distinct color change from colorless to yellow on interacting with $AcO^-$ and $F^-$ in DMSO and mixed DMSO/$H_2O$. Also, the fluorescence enhancement of L was observed upon addition of $AcO^-$ and $F^-$. MTT assay reveals that both the probe and the concentration of $F^-$ used proved non-toxic to the HeLa cell line. Although water medium compete with the anion sensing ability of L, however, we observed a slight increased cellular fluorescence when $F^-$ ions were added to HeLa cells containing L.

**Acknowledgments**
Authors are thankful to Dr Heung-Jin Choi, Department of Applied Chemistry, Kyungpook National University, Daegu, South Korea for providing necessary facilities for conducting the NMR titration experiments. This work was made possible by a grant from the DST, New Delhi (SR/S1/IC-54/2012).

## Notes and references

1. R. M. Duke, E. B. Veale, F. M. Pfeffer, P. E. Kruger and T. Gunnlaugsson, *Chem. Soc. Rev.*, 2010, **39**, 3936-3953.
2. D. G. Cho and J. L. Sessler, *Chem. Soc. Rev.*, 2009, **38**, 1647-1662.
3. P. A. Gale, N. Busschaert, C. J. Haynes, L. E. Karagiannidis and I. L. Kirby, *Chem. Soc. Rev.*, 2014, **43**, 205-241.
4.H. T. Ngo, X. Liu and K. A. Jolliffe, *Chem. Soc. Rev.*, 2012, **41**, 4928-4965.
5. M. E. Moragues, R. Martinez-Manez and F. Sancenon, *Chem. Soc. Rev.*, 2011, **40**, 2593-2643.
6. D. Sharma, S. K. Ashok Kumar and S. K. Sahoo, *Tetrahedron Lett.*, 2014, **55**, 927-930.
7. D. Sharma, S. K. Sahoo, S. Chaudhary, R. K. Bera and J. F. Callan, *Analyst*, 2013, **138**, 3646-3650.
8. K. N. Farrugia, D. Makuc, A. Podborska, K. Szacilowski, J. Plavec and D. C. Magri, *Org. Biomol. Chem.*, 2015, **13**, 1662-1672.
9. D. Sharma, A. Moirangthem, S. M. Roy, A. S.K. Kumar, J. P. Nandre, U.D. Patil, A. Basu and S. K. Sahoo, *J. Photochem. Photobiol., B*, 2015, **148**, 37-42.
10. M. Cametti and K. Rissanen, *Chem. Soc. Rev.*, 2013, **42**, 2016-2038.
11. C. Suksai and T. Tuntulani, *Chem. Soc. Rev.*, 2003, **32**, 192-202.
12. E. W. Yemeli Tido, E. J. M. Vertelman, A. Meetsma and P. J. van Koningsbruggen, *Inorg. Chim. Acta*, 2007, **360**, 3896-3902.
13. H. A. Benesi and J. H. Hildebrand, *J. Am. Chem. Soc.*, 1949, **71**, 2703-2707.
14. M. J. Frisch, G. W. Trucks, H. B. Schlegel, G. E. Scuseria, M. A. Robb, J. R. Cheeseman, G. Scalmani, V. Barone, B. Mennucci, G. A. Petersson, H. Nakatsuji, M. Caricato, X. Li, H. P. Hratchian, A. F. Izmaylov, J. Bloino, G. Zheng, J. L. Sonnenberg, M. Hada, M. Ehara, K. Toyota, R. Fukuda, J. Hasegawa, M. Ishida, T. Nakajima, Y. Honda, O. Kitao, H. Nakai, T. Vreven, J. A. Montgomery Jr., J. E. Peralta, F. Ogliaro, M. J. Bearpark, J. Heyd, E. N. Brothers, K. N. Kudin, V. N. Staroverov, R. Kobayashi, J. Normand, K. Raghavachari, A. P. Rendell, J. C. Burant, S. S. Iyengar, J. Tomasi, M. Cossi, N. Rega, N. J. Millam, M. Klene, J. E. Knox, J. B. Cross, V. Bakken, C. Adamo, J. Jaramillo, R. Gomperts, R. E. Stratmann, O. Yazyev, A. J. Austin, R. Cammi, C. Pomelli, J. W. Ochterski, R. L. Martin, K. Morokuma, V. G. Zakrzewski, G. A. Voth, P. Salvador, J. J. Dannenberg, S. Dapprich, A. D. Daniels, Ö. Farkas, J. B. Foresman, J. V. Ortiz, J. Cioslowski and D. J. Fox, Gaussian 09, (2009) Gaussian, Inc., Wallingford, CT, USA.
15. L. Gai, J. Mack, H. Lu, T. Nyokong, Z. Li, N. Kobayashi and Z. Shen, *Coord. Chem. Rev.*, 2015, **285**, 24-51.

## Graphical abstract